



## Green Synthesis and Characterization of ZnS nanoparticles

Senapati U.S.<sup>1</sup>, Jha D.K.<sup>2</sup> and Sarkar D.<sup>3</sup>

<sup>1</sup>Department of Physics, Handique Girls' College, Guwahati, INDIA

<sup>2</sup>Department of Botany, Gauhati University, Guwahati, INDIA

<sup>3</sup>Department of Physics, Gauhati University, Guwahati, INDIA

Available online at: [www.isca.in](http://www.isca.in)

Received 3<sup>rd</sup> June 2013, revised 11<sup>th</sup> July 2013, accepted 31<sup>st</sup> July 2013

### Abstract

The development of green synthesis route through biological method for the synthesis of nanoparticles using plants have received attention in the recent times as it is environment friendly and economical method. ZnS nanoparticles have been prepared using glucose both as capping agent and stabilizer. The obtained ZnS nanoparticles are studied by X-ray diffraction (XRD), Energy dispersive analysis of X-rays (EDAX), Scanning electron microscopy (SEM), Transmission electron microscopy (TEM), Selected area electron diffraction (SAED), UV-vis optical absorption, Photoluminescence techniques (PL) and Fourier Transform Infrared Spectroscopy (FTIR). The mean particle size of the ZnS nanoparticles is found to be 5.8 nm. The XRD analysis confirms the cubic and crystalline nature of the synthesized sample which is in good agreement with SAED pattern. Also, EDAX pattern confirms the presence of Zinc and Sulfur. UV-vis spectra show that the absorption peaks exhibit blue shift from the bulk. The PL investigation revealed the recombination mechanism in ZnS nanoparticles. FTIR spectra confirm the presence of glucose as capping agent.

**Keywords:** Green synthesis, glucose, ZnS, XRD, TEM, FTIR

### Introduction

Last two decades have witnessed a rapid advancement in various techniques for the fabrication of nanoparticles. Among various classes of nanoparticles, II-VI class inorganic semiconductor nanomaterials like CdS, ZnS, CdSe emerged as important materials for the applications in optoelectronics devices. ZnS is extensively studied as it has numerous applications to its credit. There are various chemical based methods available for the synthesis of ZnS nanomaterials<sup>1,2</sup>. But there is a growing concern towards use of these chemicals as they are reported to be very toxic for the environment. Apart from the toxicity, these chemical based methods are also not cost effective, a major disadvantage for synthesis of nanoparticles at the industrial scale. Due to these problems, various eco-friendly approaches for the synthesis of ZnS nanoparticles are being adopted<sup>3</sup>. Among them, plants and plant extracts seem to be the best option as Plants are nature's "chemical factories". They are cost efficient and require little or no maintenance. A vast repertoire of secondary metabolites is found in all plants which possess red ox capacity and can be exploited for biosynthesis of nanoparticles. As a wide range of metabolites are presented in the plant, the nanoparticles produced by using plants are more stable and the rate of synthesis is faster in comparison to microorganism.

Glucose is a simple monosaccharide found in plants whose five hydroxyl groups are arranged in a specific way along its six-carbon backbone. The use of carbohydrates for the synthesis of nanomaterials has recently become an active research area. Gole

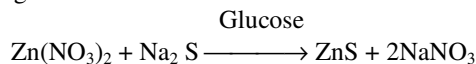
A et al used glucose as a reductant to prepare gold nanoparticles<sup>4</sup>. Raveendran P et al used D-glucose as the reducing agent and starch as a capping agent to prepare Ag nanoparticles<sup>5</sup>. Huang et al used chitosan and herparin as reducing and stabilizing agent for the synthesis of Au and Ag nanoparticles respectively<sup>6</sup>. Power M. J. et al and Bansal P. et al used glucose as a capping agent for the synthesis of CdS<sup>7,8</sup>. We report a simple and economical method for the preparation of ZnS nanoparticles using glucose as a capping agent. Glucose has been selected as the capping agent because it is abundant, natural, renewable and biodegradable. Since it is biodegradable, it may also help in reducing cytotoxicity problem of nano materials, a major limitation for their biological applications and could extend the applications of ZnS nanoparticles to food and pharmaceutical product.

### Material and Methods

Zn(NO<sub>3</sub>)<sub>2</sub> and Na<sub>2</sub>S are used as Zinc source and Sulphur source respectively. Zn (NO<sub>3</sub>)<sub>2</sub>, Na<sub>2</sub>S and glucose are obtained from Merck Specialities Private Ltd. and Qualigens fine chemicals respectively. These are of high purity and used without any future purification.

In Zn (NO<sub>3</sub>)<sub>2</sub>(1M) solution, Na<sub>2</sub>S (1M) solution is added drop wise with continuous stirring. A white coloured solution is formed which is further shaken on a magnetic stirrer for 15 hours. Now, 1.0M glucose solution is added drop wise in this white coloured solution. The resultant solution is heated and incubated at 70°C for more than 6 hours. Precipitates obtained

are centrifuged with 2,000 rpm for 15 mints. The final product is dried at 50°C for 4 hours and then crushed to fine powder. The Synthesis process can be summarized by the chemical equation given below:



## Results and Discussion

**Structural Studies:** The XRD pattern of the synthesized ZnS nanoparticles is shown in figure-1. Three broad peaks are observed in the diffractogram at around 28.32°, 47.73°, 56.50° corresponds to (111), (220) and (311) planes of cubic ZnS respectively. The presence of broad peaks in XRD implies presence of nanoparticles<sup>9</sup>. The average crystallite size is calculated using Debye-Scherrer formula<sup>10</sup>  $D = K\lambda/\beta\cos\theta$ , where D is the crystallite size, K is the geometric factor (0.9),  $\lambda$  is the X-ray wave length (1.54Å),  $\beta$  is the full width at half maxima (FWHM) of the diffraction peak (in radian) and  $\theta$  is the diffraction angle. The calculated crystallite size from the prominent (111) plane is found to be 5.26nm. The FWHM of the XRD peaks may also contain contributions from lattice strain<sup>11</sup>. Therefore, the average strain of the ZnS nanoparticles is calculated using Stokes-Wilson equation<sup>12</sup>  $\epsilon_{\text{str}} = \beta\cot\theta / 4$ , where  $\beta$  is the FWHM and  $\theta$  is the diffraction angle.

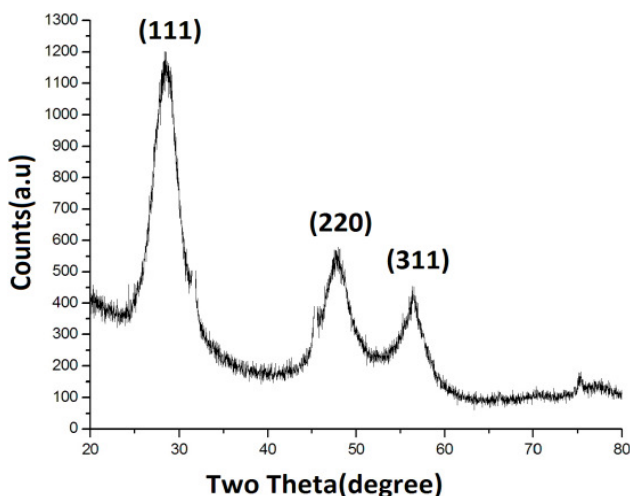


Figure-1  
XRD Spectra of ZnS nanoparticles

The dislocation density ( $\delta$ ) which represents the amount of defects in the sample is calculated using the relation<sup>13</sup>  $\delta = 1/D^2$ , where D is the average crystallite size. The d- spacing is calculated using the relation<sup>14</sup>  $d_{hkl} = n\lambda / 2\sin\theta$ .

The lattice constant is estimated from the intercept of the Nelson- Riley plot which is a graph of the calculated values of lattice constant for different planes versus the error function given by<sup>15</sup>

$$f(\theta) = \frac{1}{2} \left( \frac{\cos^2 \theta}{\sin \theta} + \frac{\cos^2 \theta}{\theta} \right)$$

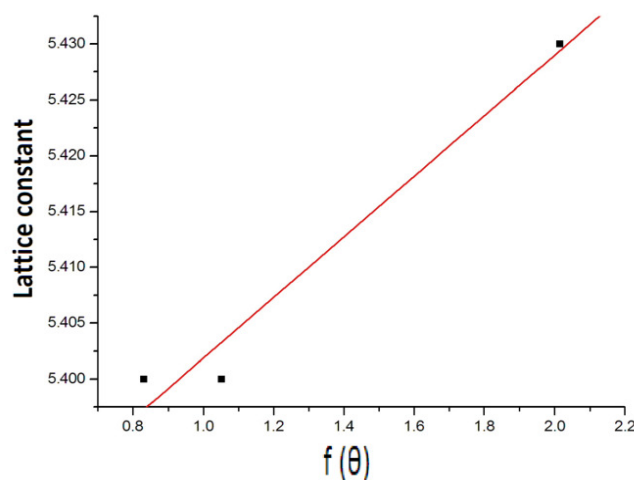


Figure-2  
Nelson- Riley plot of nanocrystalline ZnS sample

The value obtained from N-R plot is more or less free from systematic errors. The calculated structural parameters are given in table-1.

**SEM and EDAX Study:** Figure-3A shows the SEM picture of the synthesized ZnS. From this figure well structured and crystalline grains are observed. The EDAX pattern shown in Figure-3B confirms the presence of Zinc and Sulphur. Other signals including C and O are recorded possibly due to the elements present in glucose.

Table-1  
Structural Parameters of ZnS nanoparticles

2 $\theta$ (degree)	Plane(hkl)	Interplaner Spacing 'd'(Å <sup>0</sup> )	Lattice Constant 'a'(Å <sup>0</sup> )	FWHM(rad)	Average Crystallite Size D(nm)	Dislocation density $\delta$ (lines/m)	Average Strain( $\epsilon_{\text{str}}$ )
28.32	(111)	3.14		0.044			
47.73	(220)	1.91	5.37	0.023	5.26	$8.1 \times 10^{16}$	$43 \times 10^{-3}$
56.50	(311)	1.63		0.031			

**TEM Study:** Figure-4 Shows the TEM micrograph of ZnS nanoparticles. The micrograph shows that the nanoparticles are uniformly distributed and are almost spherical in shape. The mean particle size estimated from the particle size histograms is 5.83nm. The SAED pattern shown inset of the Figure-4 shows concentric rings. The rings have been indexed to (111), (220) and (311) planes of the cubic ZnS phase which correspond to  $d(111) = 3.1114\text{\AA}$ ,  $d(220)=1.904\text{\AA}$  and  $d(311)=1.6277\text{\AA}$  respectively, confirming the presence of cubic phase of ZnS crystal<sup>16</sup>.

**UV-Visible Spectra:** Figure- 5(a) shows UV-Vis spectra of ZnS nanoparticles. The sample shows a strong absorption below

300nm. The blue shift of absorption edge compared to bulk ZnS explains the quantum confinement effect of ZnS nanoparticles. The band gap energy of the ZnS nanoparticles can be evaluated from the UV-Vis spectra by using the relation<sup>17</sup>:  $(\alpha h\nu) = A(h\nu - E_g)^n$  where,  $\alpha$  is the absorption coefficient,  $h\nu$  is the incident photon energy,  $A$  is a constant and  $E_g$  is the band gap energy of the material. The exponent  $n$  depends on the type of the transition. Here, the transitions are direct so we take  $n=1/2$ .

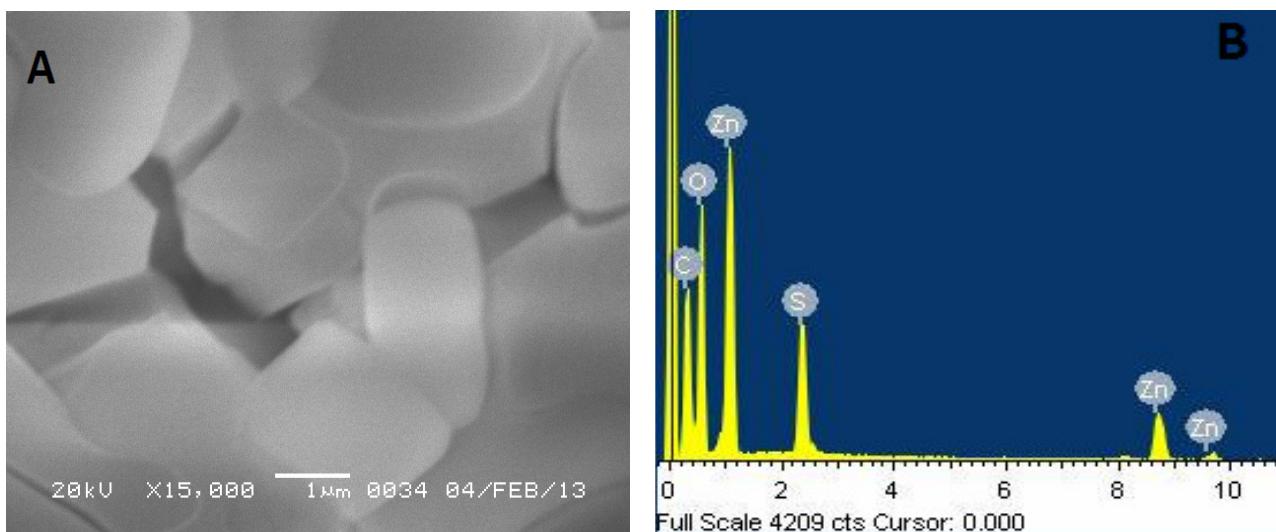


Figure-3  
 A SEM picture, B Energy dispersive X-ray analysis (EDAX) of ZnS nanoparticles

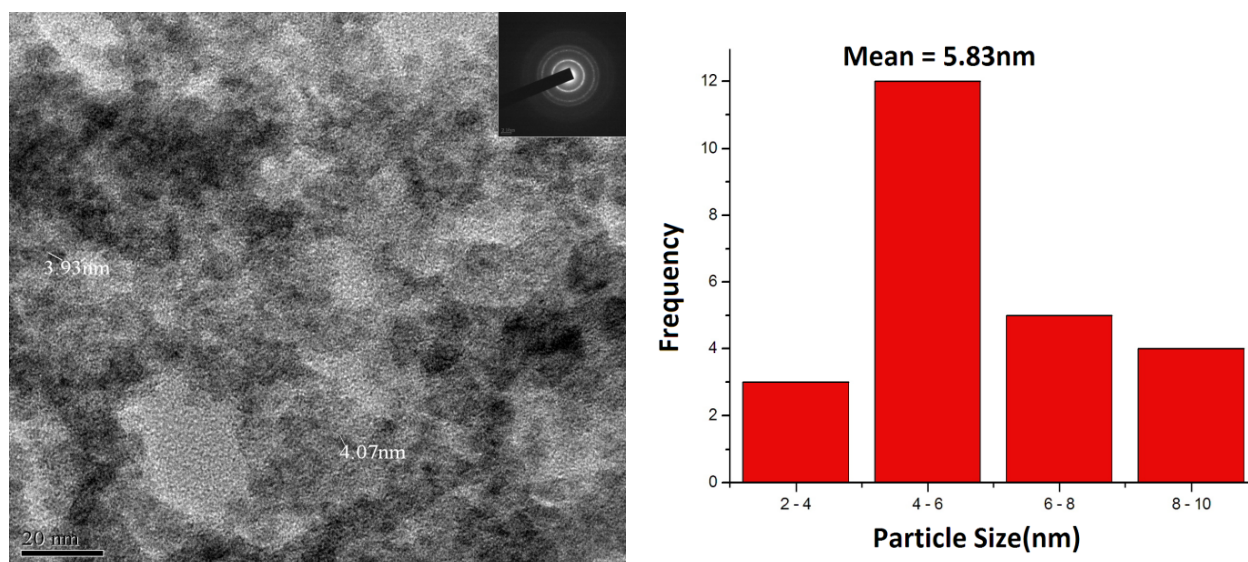


Figure-4  
 TEM micrograph of the synthesized ZnS nanoparticles with their particle size distribution

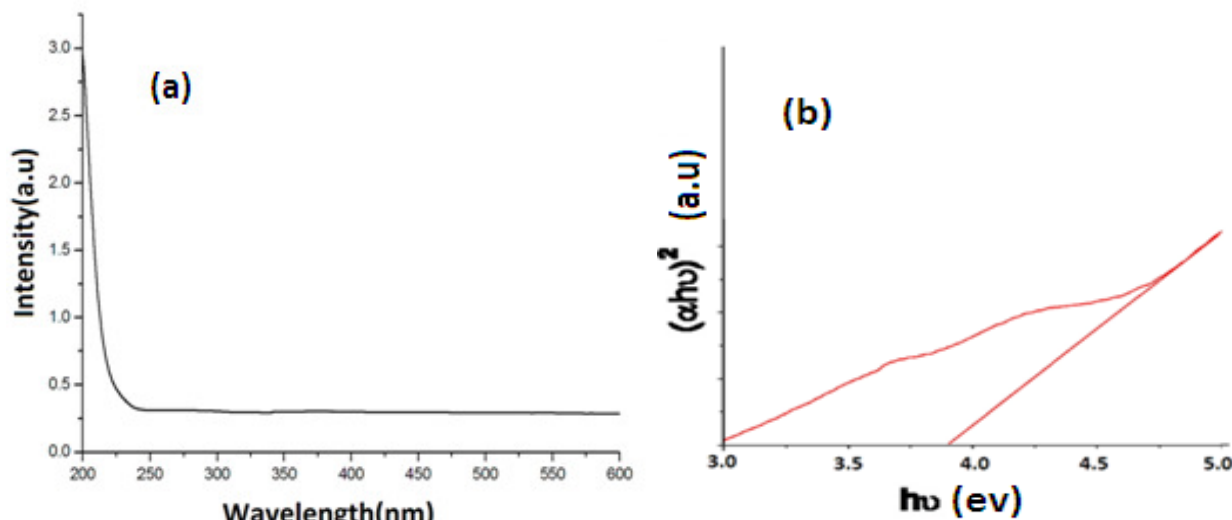


Figure-5  
(a) UV-Vis spectra and (b) Tauc plot of ZnS nanoparticles

The band gap energy is calculated by extrapolating the linear portions of the  $(\alpha hv)^2$  vs  $hv$  graph on the  $hv$  axis to  $\alpha=0$ . The obtained band gap energy value is given in table-2.

From the band gap value of nanoparticle and bulk, the particle size is calculated using the equation<sup>18</sup>:

$$\Delta E = \frac{h^2}{8r^2} \left( \frac{1}{m_e^*} + \frac{1}{m_h^*} \right) - \frac{1.8e^2}{4\pi\epsilon_0\epsilon_r}$$

Where,  $\Delta E$  is the blue shift of the band gap,  $m_e^*$  is the effective mass of electron,  $m_h^*$  is the effective mass of hole,  $r$  is the radius of the particle,  $\epsilon_r$  is the dielectric constant and  $\epsilon_0$  is the permittivity of free space. The first term indicates the confinement effect and the second term is the coulomb term. In the present case, the second term is small due to the strong confinement and can be neglected. The calculated particle size is given in Table-2.

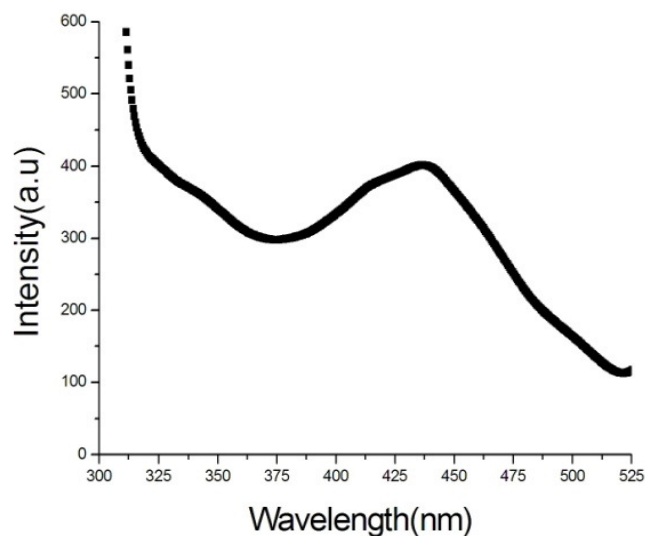


Figure-6  
Photoluminescence Spectra of ZnS nanoparticles

Table-2  
Optical band gap, blue shift and particle Size of the ZnS nanoparticles using 1.0M glucose

Optical band gap(eV)	Blue Shift $\Delta E$ (eV)	Particle Size from(nm)		
		UV	XRD	TEM
3.8	0.2	4.46	5.26	5.83

**Photoluminescence (PL) Study:** The room temperature photoluminescence spectrum of ZnS sample for excitation wavelength of 280nm is shown in figure-6. This shows peak centred at 437nm. Appearance of the broad peak centred at 437nm is due to the zinc vacancies present near the valance band<sup>19</sup>.

**FTIR Study:** FTIR study is carried out to identify the capping of the particles by glucose. The very strong peak at  $1111\text{cm}^{-1}$  may be contributed by - C - O groups of glucose. The peaks at  $3500\text{cm}^{-1}$  is very broad and strong and can be assigned to the - OH groups from glucose. The IR study confirms the presence of -C-O and -OH groups of glucose have a strong ability to bind metal. So we can infer that ZnS nanoparticles are encapsulated by glucose. It has been earlier reported that gluconic acid derived from glucose can cap the nanoparticles<sup>20</sup>.

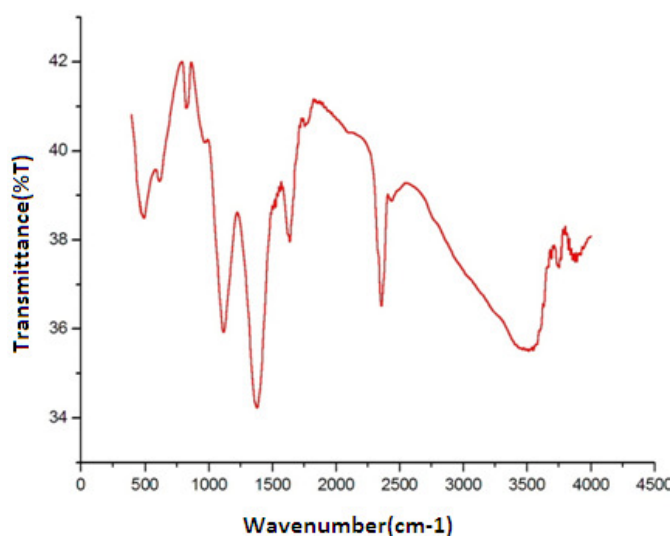


Figure-7

FTIR Spectrum of ZnS nanoparticles. The inset shows structure of D-Glucose

## Conclusion

ZnS nanoparticles have been successfully synthesized by green route with average particle size of 5.83 nm using glucose as capping agent. XRD and SAED patterns confirm the cubic crystalline structure of ZnS. EDAX analysis confirms the presence of Zinc and Sulphur. The morphology of the particles has been identified from the SEM and TEM analysis and reveals a spherical shape. The UV-vis absorption peak exhibits blue shift from the bulk. PL spectrum shows a broad peak at 437nm. The FTIR study confirms that -C-O and -OH groups of glucose could bind with ZnS nanoparticles.

## Acknowledgments

Authors gratefully acknowledge Institutional Biotech Hub, Handique Girls' College, Guwahati for giving Laboratory facilities. We also acknowledge IASST, Guwahati for XRD measurements, Department of Chemistry, Gauhati University for UV-Visible, PL and FTIR measurements, SAIF, NEHU, Shillong for SEM and TEM measurements and Department of Physics, Tezpur University for EDAX measurements.

## References

1. Baishya U. and Sarkar D., ZnS nanocomposite formation: Effect of ZnS source concentration ratio, *Indian J. of pure & Applied Physics*, **49**, 186-189 (2011)
2. Gosh Gopa. Naskar Milan Kanti., Patra Amitava. and Chatterjee Minati., Synthesis and characterization of PVA-encapsulated ZnS nanoparticles, *optical Materials*, **28**, 1047-1053 (2006)
3. Bai H.J., Zhang Z.M. and Gong J., Biological Synthesis of Semiconductor Zinc Sulfide nanoparticles by immobilized Rhodobacter Sphaeroides, *Biotechnol Letter*, **28**, 1135-1139 (2006)
4. Gole A., Kumar A., Phadtare S., Mandal A.B. and Sastry M., Glucose induced in-situ reduction of Chloroaurate ions entrapped in a fatty amine film: formation of gold nanoparticle-lipide Composites, *Phys Chem Comm*, **19**, 1-4 (2001)
5. Raveendran P., Fu J. and Wallen S., Completely "green" synthesis and stabilization of metal nanoparticles, *J.Am.Chem.Soc*, **125**, 13940-1 (2003)
6. Huang H. and Yang X., Synthesis of Polysaccharide-Stabilized gold and silver nanoparticles : a green method, *Carbohydr. Res.*, **339**, 2627-2631 (2004)
7. Pawer M.J. and Chaure S.S, Synthesis of CdS nanoparticles using Glucose as a capping agent, *Chalcogenide Letters*, **12**, 689-693 (2009)
8. Bansal P., Jaggi N. and Rohilla S.K., "Green" Synthesis of CdS nanoparticles and effect of capping agent concentration on crystallite size, *Res.J.Chem.Sci.*, **2**, 69-71 (2012)
9. Bodo Bhaskarjyoti and Kalita P.K. , Chemical Synthesis of ZnS:Cu Nanosheets, *AIP Conf. Proceed*, **1276**, 31-36 (2010)
10. Ramasamy V., Praba K. and Murugadoss G., Study of optical and thermal properties in nical doped ZnS nanoparticles using Surfactants, *Superlattices and Microstructures* , **51**, 699-714 (2012)
11. John Rita and Florence S. Sasi, Structural and optical properties of ZnS nanoparticles synthesized by solid state reaction method, *Chalcogenide Letters*, **6**, 535-539 (2009)
12. Begum Anayara, Hussain Amir and Rahman Atowar, Effect of deposition temperature on the structural and optical properties of chemically prepared nanocrystalline lead selenide thin films, *Beilstein J.Nanotechnol.*, **3**, 438-443 (2012)
13. Dhanam M., Kavitha B. and Velumani S., An investigation on Silar Cu(In<sub>1-x</sub> Al<sub>x</sub>)Se<sub>2</sub> thin films, *Mat.Sc. and Eng. B*, **174**, 209-215 (2010)
14. Dhanam M., Kavitha B., Jose Neetha. and Devasia Dheera. P., Analysis of ZnS nanoparticles prepared by surfactant micelle-temperature inducing reaction, *Chalcogenide Letters*, **6**, 713-722 (2009)
15. Sarma K., Sarma R. and Das H.L., Structural Characterization of thermally evaporated CdSe thin films, *Chalcogenide Letters*, **5**, 153-163 (2008)
16. Hudlikar H., Joglekar S., Dhaygude M. and Kodam K., Latex - mediated synthesis of ZnS nanoparticles: green synthesis approach, *J.Nanopart.Res.*, **14**, 865 (2012)

17. Devi B.S. Rema, Raveendran R. and Vaidyan A.V., Synthesis and Characterization of Mn<sup>2+</sup>- doped ZnS nanoparticles, *Pramana-J.Phys.*, **68**, 679-687 (2007)
18. Brus L.E., Electron-electron and electron-hole interactions in small Semiconductor Crystallites: The Size dependence of the lowest excited electronic State, *J.Chem.Phys*, **80**, 4403-4409 (1984)
19. Denzler D., Olschewski M. and Sattler K., Luminescence Studies of localized gap States in Colloidal ZnS nanoparticles, *Journal of Applied Physics*, **84**, 2841 (1998)
20. Amany A., El-Kleshien and Sanaa F.Gad El-Rab, Effect of reducing and Protecting agents on Size of Silver nanoparticles and their anti-bacterial activity, *Der Pharma Chemica*, **4**, 53-65 (2012)